Grand canonical simulation of phase behaviour in highly size-asymmetrical binary fluids

Douglas J. Ashton[1] and Nigel B. Wilding[1]

[1] *Department of Physics, University of Bath, Bath BA2 7AY, United Kingdom.*

We describe a Monte Carlo scheme for the grand canonical simulation study of fluid phase equilibria in highly size-asymmetrical binary mixtures. The method utilizes an expanded ensemble in which the insertion and deletion of large particles is accomplished *gradually* by traversing a series of states in which a large particle interacts only partially with the environment of small particles. Free energy barriers arising from interfacial coexistence states are surmounted with the aid of multicanonical preweighting, the associated weights being determined from the transition matrix. As an illustration, we present results for the liquid-vapour coexistence properties of a Lennard-Jones binary mixture having a 10 : 1 size ratio.

I. INTRODUCTION

Fluid mixtures comprising two or more particle species of disparate sizes are common in soft condensed matter [1]. A prime example is a colloidal dispersion to which much smaller particles have been added such as non-absorbing polymers [2–4] or charged nanoparticles [5]. Interest in such systems stems from the fact that by judicious choice of the small component, one can potentially control the equilibrium and dynamical properties of the large component, giving rise to a rich assortment of novel phenomena and material properties [2, 6]. Given, however, the wide variety of small particles that one might conceivably choose to add, the experimental task of characterizing the range of possible behaviour is considerable. With this in mind there has been much interest in deploying statistical mechanics and computer simulation to *predict* the properties of such mixtures.

In this paper we shall focus on the problem of obtaining the equilibrium phase behaviour of models of highly size-asymmetrical mixtures. Direct analytical assaults on such systems are generally complicated by the disparity in particle length scales [7]. To make progress, a widely practiced simplifying strategy is to try to map the true two-component mixture onto a single component system comprising solely the colloid particles. These are assumed to interact via an *effective* potential which is supposed to represent the net effect of the bare colloid-colloid interactions plus the additional interactions mediated by the small particles. Arguably the most successful example of such an approach pertains to particles that interact as hard spheres – a situation which can be realized experimentally to a good approximation in colloid-polymer mixtures [8]. Here the effective interaction is the celebrated "depletion" potential describing the interaction between two hard sphere colloids immersed in a "sea" of small hard spheres [9]. In seminal work, Bob Evans and coworkers have contributed much insight into this situation by tracing out the degrees of freedom associated with the small particles in order to produce an explicit expression for the depletion potential parameterized by the particle size ratio and the volume fraction of small particles. This not only provides valuable information on the nature of the colloidal interactions, but also serves as a basis for theoretical and simulation investigations of the phase behaviour of the effective one component system [10–12].

Whilst impressive progress has been made in obtaining accurate effective one-component potentials, at present they are largely limited to underlying interactions of the hard sphere form [1]. Moreover, because effective potentials are usually derived in the limit of low density of large particles, there are concerns about their accuracy at high densities where many body effects are significant. Ideally then, one should like to be able to tackle the full two component system and treat arbitrary interactions between the particle species. Achieving this analytically still seems some way off, making it tempting to appeal to computer simulation for help. Unfortunately, simulations of highly size asymmetric mixtures encounter their own problems: the relevant physics is controlled by the length scale of the large particles, but attempts to relax these particles are often frustrated by the presence of the small ones. For instance grand canonical Monte Carlo simulations – the method of choice for studies of fluid phase transitions [13] – suffer an unfeasibly small acceptance rate for insertions of large particles. Similarly in Molecular Dynamics an impractically small timestep is mandated by the need to avoid high energy overlaps between large and small particles.

In this paper we describe a tailored Monte Carlo simulation scheme that circumvents the principal drawbacks of traditional approaches. The essential idea is to treat both species grand canonically, but to ease the sampling bottleneck for insertions (and deletions) of large particles by performing these – not in a single Monte Carlo step – but *gradually*. In practice this is achieved by permitting the system to traverse (in a stochastic fashion) a prescribed set of states (or "stages") that interpolate between the limits of a large particle being fully present and fully absent from the system. This idea of staged insertion has been around for some time, principally in the context of chemical potential measurements for dense fluids and complex molecules using the Widom formula [14–19]. It has been recently revisited in the context of optimizing expanded open ensembles by Escobedo [20]

and by Shi and Maginn [21]. However, to our knowledge it has not been used to calculate the phase behaviour of a model asymmetric mixture at large ratios of the component sizes.

Whilst our method is quite capable of treating both large and small particles on an equal footing when determining the phase behaviour of the mixture, the perspective we adopt in the present paper is one inspired by the colloidal systems discussed above. Specifically, we shall focus primarily on the phase coexistence properties of the large species (colloids), the role of the small particles being assumed to modify the effective interactions between the large ones. Hence the phase diagram that we shall present is a single component (large species) projection of the full phase diagram, this being obtained at constant reservoir volume fraction of the small species.

II. METHOD

In this section we begin by outlining the statistical mechanical basis to the staged insertion method for a highly size asymmetric binary mixture. Thereafter we discuss implementation issues, taking as an example the case of a Lennard-Jones (LJ) mixture.

A. Statistical mechanics

Consider a binary mixture comprising N particles, N_l of which are 'large' (l) and N_s of which are 'small' (s), all contained in a volume V at temperature T. Particles are identified via an index $1 \leq i \leq N$, and a species label $\gamma_i = l, s$, and we write the internal energy as

$$\Phi = \sum_{i=1}^{N} \sum_{j=i+1}^{N} \phi_{\gamma_i,\gamma_j}(\mathbf{q}_i, \mathbf{q}_j) \ , \qquad (1)$$

where ϕ_{γ_i,γ_j} is the pair potential for particles i and j of species γ_i and γ_j, located at position vectors $\mathbf{q}_i$, and $\mathbf{q}_j$ respectively.

Let us now augment this system with an additional 'ghost' (G) large particle having position vector $\mathbf{q}_G$. The ghost particle is taken to interact normally with other large particles, but differently with small particles. To deal with this, it is more convenient to associate separate indices k and m with the N_l large and N_s small particles respectively, and write the interaction of the ghost particle as

$$\Phi_G = \sum_{k=1}^{N_l} \phi_{ll}(\mathbf{q}_k, \mathbf{q}_G) + \sum_{m=1}^{N_s} \tilde{\phi}_{ls}^{(n)}(\mathbf{q}_m, \mathbf{q}_G) \ . \qquad (2)$$

Here $\tilde{\phi}_{ls}^{(n)}$ describes the interaction between the ghost large particle and a small particle. This is modified with respect to the standard large-small interaction by the dependence on a discrete stochastic macrovariable $n = 0 \ldots M-1$. The role of n is to index the stages that specify the degree of coupling between the ghost and the small particles. Fluctuations in n forwards or backwards across its range result in the gradual insertion or deletion of a large particle (Fig 1). To be more specific, we let $n = 0$ correspond to N_l large particles, while $n = M$ corresponds to $N_l + 1$. Intermediate values of $n = 1 \ldots M-1$ represent a system of N_l large particles plus a ghost particle. Thus transitions $n = 1 \to 0$ correspond to the deletion of the ghost particle from the system, while $n = M-1 \to M$ correspond to it turning into a fully interacting (ie. standard) large particle. In this sense the $n = M$ state for a system of N_l large particles and the $n = 0$ state for a system of $N_l + 1$ large particles are equivalent.

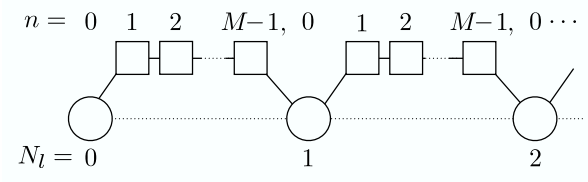

FIG. 1. Schematic showing how each integer value of the large particle number N_l is expanded into M stages, each of which is indexed by the macrovariable n.

The internal energy of the augmented system is $\Phi'(\{\mathbf{q}\}_l, \{\mathbf{q}\}_s, q_G, n) = \Phi + \Phi_G$ and the associated 'expanded' [22] canonical ensemble has the partition function $Z'(N_l, N_s, V, T, n)$, where

$$Z' = \prod_{k=1}^{N_l} \prod_{m=1}^{N_s} \int d\mathbf{q}_k \int d\mathbf{q}_m \int d\mathbf{q}_G \exp[-\beta\Phi'], \qquad (3)$$

with $\beta = 1/k_B T$. In the present work, we shall be concerned with the measured form of the *grand canonical* (GC) ensemble probability distribution of the fluctuating number of large particles, $p(N_l|\mu_l, \mu_s, V, T)$, where μ_s and μ_l are the chemical potentials of the small and large species respectively. This is obtainable from measurements of the joint distribution $p(N_l, n|\mu_l, \mu_s, V, T)$ conducted within the expanded GC ensemble, which is defined via a weighted sum of the expanded canonical ensemble partition function Z':

$$p(N_l, n) \simeq \sum_{N_s=0}^{\infty} Z' \exp\left[\beta(N_l\mu_l + N_s\mu_s)\right] \ . \qquad (4)$$

Here $\simeq$ means up to an arbitrary normalization constant and (for brevity) we have omitted combinatorical and volume factors. $p(N_l|\mu_l, \mu_s, V, T)$ follows from Eq. 4 by picking out those macrostates from the expanded ensemble having $n = 0$, ie. that correspond to the physical

states in which no ghost particles are present in the system:

$$p(N_l) = \frac{1}{\mathcal{Z}} \sum_{N_s=0}^{\infty} \sum_{n=0}^{M-1} Z' \exp\left[\beta(N_l\mu_l + N_s\mu_s)\right] \delta_{n,0} \quad (5)$$

where

$$\mathcal{Z} = \sum_{N_l=0}^{\infty} \sum_{N_s=0}^{\infty} \sum_{n=0}^{M-1} Z' \exp\left[\beta(N_l\mu_l + N_s\mu_s)\right] \delta_{n,0} \quad (6)$$

is the grand partition function.

In the present work we shall seek to obtain $p(N_l, n)$ at state points (μ_l, μ_s, T) for which its form may vary over many decades. Variations on such a scale preclude direct measurements of $p(N_l, n)$ unless special biasing techniques are deployed to facilitate sampling of the regions of intrinsically low probability. To this end we utilize multicanonical preweighting [23], specifying a sampling distribution

$$\hat{p}(N_l, n|w) \simeq p(N_l, n) \exp[w(N_l, n)], \quad (7)$$

where $w(N_l, n)$ represents a set of weights defined on the discrete combinations $\{N_l, n\}$. As shall be described in Sec. II B, these weights are chosen such as to ensure approximately uniform sampling on the set. The desired form of $p(N_l)$ is regained from the measured form of $\hat{p}(N_l, n)$ by first using Eq. 7 to unfold the effects of the weights, then picking out those macrostates having $n = 0$.

B. Implementation for a binary Lennard-Jones mixture

In order to illustrate how the above formalism can be implemented in practice, we consider the case of a binary mixture of Lennard-Jones particles. Pairs of particles labelled i and j (having respective species labels γ_i and γ_j) interact via the potential

$$\phi_{ij}(r) = 4\varepsilon_{\gamma_i\gamma_j} \left[\left(\frac{\sigma_{\gamma_i\gamma_j}}{r} \right)^{12} - \left(\frac{\sigma_{\gamma_i\gamma_j}}{r} \right)^{6} \right] . \quad (8)$$

Here $\varepsilon_{\gamma_i\gamma_j}$ is the well depth of the interaction, while $\sigma_{\gamma_i\gamma_j}$ sets the range of the interaction based on the additive mixing rule $\sigma_{\gamma_i\gamma_j} = (\sigma_{\gamma_i} + \sigma_{\gamma_j})/2$, where σ_{γ_i} and σ_{γ_j} are the particle diameters. Interactions are truncated at $r_c = 2.5\sigma_{\gamma_i\gamma_j}$ and we take σ_l as our unit length scale.

We shall be concerned with state points in which the small particles occupy a relatively small fraction of the overall volume and act as a quasi-homogeneous background to the large ones. Under these circumstances, configurations of small particles can readily be sampled using a standard GC algorithm at constant chemical potential, μ_s. As is customary (in order to make contact with experimental scenarios), we choose μ_s to yield a prescribed volume fraction, η_s^r, of small particles in the *reservoir* [24]. Since we seek a quasi-uniform density of small particles, we set $\varepsilon_{ss} = \varepsilon_{ls} = \varepsilon_{ll}/10$, which ensures that the small particle reservoir fluid lies well above its own (liquid-vapour) critical temperature. In the results of Sec. III we refer to a dimensionless temperature which is defined as $T^\star = 1/(\beta\varepsilon_{ll})$.

For highly size-asymmetric mixtures, a large number of small particles are typically found within the cutoff radius $2.5\sigma_{ls}$ of each large particle. In order to locate efficiently these particles, we partition our cubic simulation box of volume $V = L^3$ into cubic cells of linear extent $2.5\sigma_{ls}$, and maintain a list of cell occupancies. Similar cells structures were employed to identify small-small and large-large interactions [25].

As described in Sec. II A, a large particle is inserted or deleted in stages by modifying its interaction with the small particles. Accordingly one must specify in advance the form of the ghost particle interaction for each stage n. Obvious candidate strategies include varying the well depth of the interaction, or its range. However, we have found that neither of these approaches operates particularly effectively in practice because of the rapid increase of the potential for distances less than that of the potential minimum. Specifically, particles whose separation is such that the interaction energy is small at one value of n can incur a very high energy penalty at a neighbouring stage. This impacts adversely on the acceptance rate, a difficulty which can only be mitigated by employing a large total number of stages M.

A superior strategy circumvents this problem by imposing a minimum on the attractive part of the interaction potential and a maximum on the repulsive part:

$$\tilde{\phi}_{ls}^{(n)}(r) = \begin{cases} \min(\phi_{ls}(r), \tilde{\phi}_{\max}^{(n)}) & r < \sigma_{ls} \\ \max(\phi_{ls}(r), \tilde{\phi}_{\min}^{(n)}) & r \geq \sigma_{ls} \end{cases} . \quad (9)$$

Each stage, n, is thus specified by a pair of parameters, $\tilde{\phi}_{\min}^{(n)}$ and $\tilde{\phi}_{\max}^{(n)}$. The form of $\tilde{\phi}_{ls}^{(n)}(r)$ for two such stages is compared schematically with the full potential $\phi_{ls}(r)$ in fig. 2.

Once the set of stages has been defined, a Monte Carlo scheme for sampling them can be implemented. Given a system of N_l large particles and a ghost particle at stage n, a proposal is made to perform a transition to an adjacent stage, $n \to n'$. This proposal is accepted or rejected according to a simple Metropolis criterion

$$p_{\rm acc} = \min\big(1, \exp\big[-\beta(\Phi_G^{(n')} - \Phi_G^{(n)}) + \Delta w\big]\big) , \quad (10)$$

where Φ_G is given by Eq. (2) and $\Delta w = w(N_l, n) - w(N_l, n')$ is the difference in multicanonical weights in the old and new states, the specification of which is discussed below. Note that special measures pertain to transitions

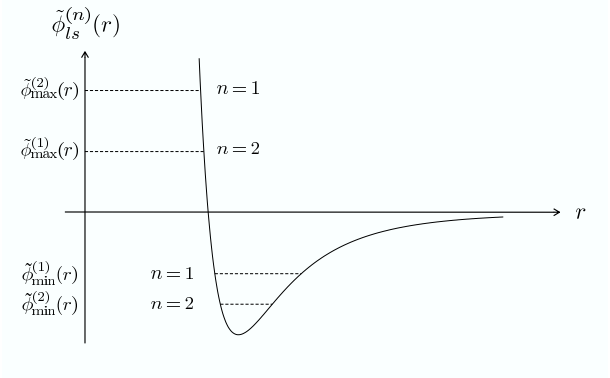

FIG. 2. Schematic form of the interaction between the ghost particle and a small particle, $\tilde{\phi}_{ls}^{(n)}(r)$ (Eq. 9) for two values of n, compared to the full LJ interaction potential between large and small particles.

that bring the ghost particle to the end of the range of n. Specifically, for a transition $n = 1 \to 0$, the ghost particle is completely removed from the system; the reverse move entails a new ghost being added at a randomly chosen location. On the other hand, when a ghost particle undergoes a transition $n = M - 1 \to M$, it becomes fully coupled to the rest of the system, $\tilde{\phi}_{ls}(r) = \phi_{ls}(r)$, and $N_l \to N_l + 1$; the corresponding reverse move entails nominating a randomly chosen large particle to become a ghost and setting $N_l \to N_l - 1$. In such circumstances the difference in weights appearing in Eq. 10 is $\Delta w = w(N_l, n) - w(N_l', n')$.

In standard GC simulation, updates that insert or remove a particle usually incorporate a factor of $e^{\beta\mu_l}V/(N_l+1)$ (insertion) or $e^{-\beta\mu_l}N_l/V$ (deletion) in $p_{\rm acc}$ to yield the correct GC equilibrium distribution. When operating in the expanded GC ensemble it is convenient (in the interests of obtaining a smooth weight function in the expanded space of N_l and n) to set the chemical potential $\mu_l = 0$ and to ignore the volume and particle number factors for the time being. The neglected factors, as well as the unfolding of the multicanonical weights (cf. Eq. 7) are easily accounted for when extracting the final GC distribution from the measured form of $\hat{p}(N_l, n)$:

$$\log p(N_l|\mu_l) \simeq \log \hat{p}(N_l, n = 0|\mu_l = 0) + \beta\mu_l N_l \qquad (11)$$
$$-w(N_l, n = 0) + N_l \log V - \log(N_l!).$$

We turn now to the matter of the choices for the number of stages M and the associated values of the stage parameters $\tilde{\phi}_{\rm min}^{(n)}$ and $\tilde{\phi}_{\rm max}^{(n)}$. This is governed by three main desiderata :

(i) The rates for transitions between neighbouring stages should be roughly equal (in both directions) in order to avoid bottlenecks in the sampling.

(ii) M should be sufficiently large to ensure a reasonably high transition rate.

(iii) The number of stages M should not be so large that the correlation time of the resulting random walk in $\{N_l, n\}$ is excessive (bearing in mind that the time to cover a given number of steps grows like the square of the number of steps).

With regard to (i), as we have chosen to implement it, staging solely influences the strength of interaction between the ghost large particle and the small particles. Hence it does nothing to ameliorate the decrease in acceptance rate that accompanies an increase in the large particle density – a situation analogous to standard GC simulations of single component fluids. Thus even if the effects of the small particles were to be offset equally for all N_l, one would still expect the transition rate to fall with increasing N_l. In such a situation, one can at best aim to avoid bottlenecks in the sampling by ensuring that (i) is satisfied *locally* in $\{N_l, n\}$. With regard to (ii) and (iii), there is in practice a tradeoff to be realized here which (in parallel with satisfying (i)) may necessitate a degree of trial and error, although more systematic approaches have been considered in the expanded ensemble literature [20]. In sec. III we consider factors affecting the choice for one practical situation.

As discussed in Sec. II A, the form of $p(N_l, n)$ may span many decades of probability and in order to sample it effectively, multicanonical preweighting is called for. This in turn requires knowledge of a set of weights, $w(N_l, n)$, that facilitate the even-handed sampling of regions of high and low probability. One choice that ensures this is $w(N_l, n) \approx -\log p(N_l, n)$ which results in a sampled distribution $\hat{p}(N_l, n)$ that is approximately flat (cf. Eq. 7) [26]. However, since $p(N_l, n)$ is just the distribution that we seek, the task of determining the weight function appears –at first sight– to be circular. Fortunately though, the situation is saved by the observation that it is possible to build up a suitable estimate of $w(N_l, n)$ from scratch via iterative means [29]. The approach we favour for doing so is based on the transition matrix Monte Carlo (TMMC) method [30–34].

TMMC works by monitoring the transitions between macrostates and using these to infer their relative probability. Once sufficient transition statistics have been collected, it is possible to construct the entire probability distribution. The starting point is the macrostate balance condition relating the equilibrium probability of two macrostates u and v to the transition rates between them:

$$p(u)W(u \to v) = p(v)W(v \to u)\ , \qquad (12)$$

where u and v are taken to represent combinations of N_l and n. The equilibrium transition rate, $W(u \to v)$ can be estimated in the course of a simulation by accumulating the acceptance probabilities for macrostate transitions into a collection matrix, $C(u \to v)$. For every proposed move, $u \to v$, the *unbiased* acceptance probability, a (calculated from Eq. 10 by assuming $\Delta w = 0$) is added to the collection matrix thus:

$$C(u \to v) \to C(u \to v) + a \tag{13}$$
$$C(u \to u) \to C(u \to u) + (1 - a)\ . \tag{14}$$

This happens regardless of whether or not the move is accepted.

The transition rates can be extracted from the collection matrix via

$$W(u \to v) = \frac{C(u \to v)}{\sum_{v'} C(u \to v')}\ , \tag{15}$$

where the sum in the denominator on the right hand side runs over all possible values of the macrovariable.

Putting the transition rates into equation (12) yields the macrostate probabilities

$$\frac{p(v)}{p(u)} = \frac{W(u \to v)}{W(v \to u)}\ , \tag{16}$$

from which the multicanonical weights follow as

$$w(u) - w(v) = -\ln \frac{W(u \to v)}{W(v \to u)}. \tag{17}$$

Since the collection matrix is concerned solely with unbiased acceptance probabilities, one is free to apply an arbitrary bias during the simulation without affecting estimates of equilibrium properties. This feature of TMMC can be exploited to provide an automated strategy for obtaining a suitable multicanonical weight function. Starting with no knowledge of the weight function, one simply updates $w(N_l, n)$ periodically via equation (17). This allows the sampling to gradually extend over the range of N_l, n, pushing progressively into regions of ever smaller probability [35]. Once the region of interest has been adequately sampled, the collection matrix provides an estimate of the requisite distribution $p(N_l, n)$ via Eq. 16. During the simulation we also sample (in list form [37]) the instantaneous values of N_l, N_s, n, together with the configurational energy Φ. This permits extrapolation of the results for $p(N_l, n)$ in temperature via standard histogram reweighting techniques [36].

III. APPLICATION TO THE LIQUID-VAPOUR TRANSITION OF A BINARY LENNARD-JONES MIXTURE

As a test of our method, we have applied it to the study of liquid-vapour phase coexistence in a LJ mixture having particle size ratio $q \equiv \sigma_{ss}/\sigma_{ll} = 0.1$ and reservoir volume fraction of the small particles $\eta_s^r = 0.01$. The simulations were performed for a cubic periodic simulation box of side $L = 7.5$, which for this η_s^r would correspond to $N_s \approx 8000$ in the absence of large particles. Since the coexistence properties of this system are known already on the basis of simulation studies using a very different approach (previously proposed by one of us [39]), there exists a convenient baseline for comparison.

	$0 \le N_l \le 130$		$N_l > 130$	
Stage, n	$\tilde{\phi}_{\min}$	$\tilde{\phi}_{\max}$	$\tilde{\phi}_{\min}$	$\tilde{\phi}_{\max}$
1	-0.5	$7.5 \to 2.7$	0	0
2	-0.8	$20 \to 16$	-0.5	7.5
3	-	-	-0.8	20

TABLE I. The stage parameters $\tilde{\phi}^{(n)}_{\min}$ and $\tilde{\phi}^{(n)}_{\max}$ (expressed in units of ϵ_{ls}) as used in the simulations. For $0 \le N_l \le 130$, two intermediates stages ($n = 1, 2$) were used (ie. $M = 3$), and $\tilde{\phi}^{(n)}_{\max}$ was varied linearly as a function of N_l between the limits shown (see text). For $N_l > 130$, three intermediate stages were used ($M = 4$) with no variation of parameters.

The choice of the stage parameters $\tilde{\phi}^{(n)}_{\min}$ and $\tilde{\phi}^{(n)}_{\max}$ was guided by the criteria set out in Sec. II B. For small values of $N_l \le 130$, only two intermediate stages were required (ie. $M = 3$) to obtain a fairly high transition rate. However, in order to maintain a roughly constant transition rate across intermediate stages for different N_l, it was found necessary to vary $\tilde{\phi}^{(n)}_{\max}$ linearly as a function of N_l between the limits shown in Table I. For $N_l > 130$ the overlap of the ghost with large particles becomes the principal ground for rejecting an insertion, and we chose to mitigate this by the introduction of an additional stage (assigned to $n = 1$) with parameters $\tilde{\phi}^{(1)}_{\min} = \tilde{\phi}^{(1)}_{\max} = 0$, thus making $M = 4$. No variation of the other stage parameters was deemed necessary in this regime, whose values for $\tilde{\phi}^{(n)}_{\min}$ and $\tilde{\phi}^{(n)}_{\max}$ are included in Table I. Across the entire range of N_l studied, the acceptance rate for transitions varied from $\simeq 30\%$ at small densities of large particle to $\simeq 5\%$ at liquid-like densities. The principal source of this variation is overlaps between the ghost particle and large particles; its magnitude compares favourably with that occurring in grand canonical studies of single component fluids over the same density range.

The simulations were initialized at the temperature $T^\star = 1.047$, close to the known critical temperature of the model [39]. At this temperature the TMMC method was used to obtain a suitable form for the multicanonical weight function and thence an estimate of the histogram $p(N_l, n)$ for $N_l = [0 : 300]$. This histogram was then reweighted in μ_l such as to satisfy the equal area criterion [38] for the two peaks in the near-coexistence form of $p(N_l)$, thereby yielding an estimate of the coexistence value of μ_l. Of course, the coexistence condition of equal pressures of the phases actually implies equal a-priori probabilities of the two phases in the space of *both* components i.e. equal integrated weight of the two peaks in the joint distribution $p(N_l, N_s)$. However, this is equivalent to equal areas under the double peaked form of either $p(N_l)$ or $p(N_s)$ that results when $p(N_l, N_s)$ is projected onto either axis. Given our viewpoint, inspired

by colloidal systems (see Sec. I), that the small particles act to modify the effective single component phase behaviour of the large ones, we focus on the forms of $p(N_l)$ at constant η_s^r.

The data accumulated at $T^\star = 1.047$ was subsequently extrapolated to the lower temperature $T^\star = 1.0$ by means of histogram reweighting, maintaining the reservoir volume fraction $\eta_s^r = 0.01$ constant in the process (which necessitates a concommitant re-tuning of μ_s). The resulting form of $p(N_l, n)$ provided a suitable multicanonical weight function for a new run at this lower temperature. By iterating this process we were able to step along the coexistence curve without the need to ever recalculate a multicanonical weight function from scratch. Further details of this strategy for mapping liquid-vapour coexistence lines are described in ref. [37].

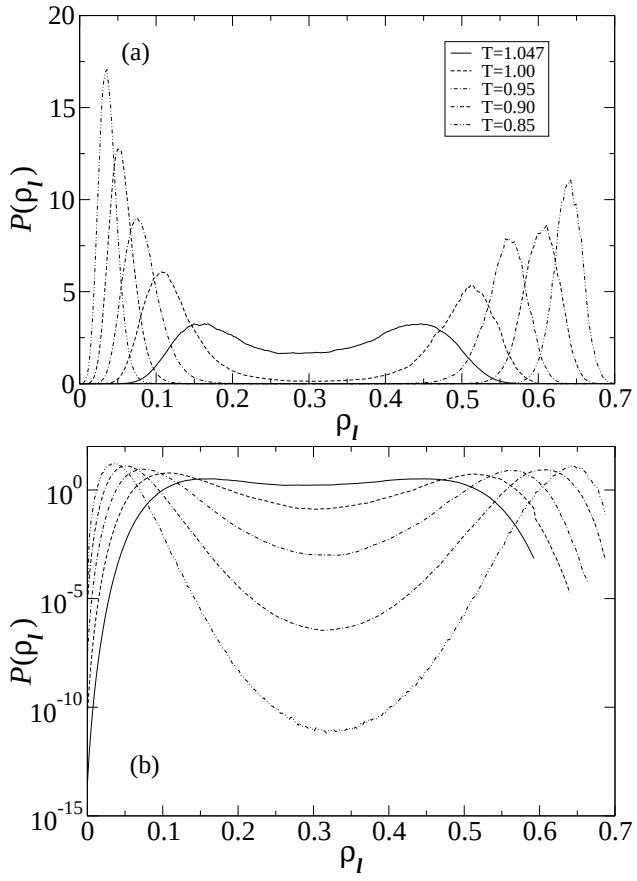

FIG. 3. **(a)** Estimates of the coexistence forms of $P(\rho_l)$ for $\eta_s^r = 0.01$ obtained using the methods described in the text. Data are shown for $T^\star = 1.047$ (criticality), $1.0, 0.95, 0.90, 0.85$. **(b)** The same data expressed on a log scale.

Fig. 3 presents our resulting estimates of the coexistence forms of $p(\rho_l)$ with ($\rho_l = N_l/V$) at various temperatures. Not surprisingly, the distributions exhibit behaviour which is qualitatively similar to that of a single component fluid [13]. An estimate of the corresponding liquid-vapour binodal can be extracted from the distributions (by averaging the density under each peak) and is shown in Fig. 4(a). Also included in Fig. 4(a) is the binodal for the single component LJ fluid determined in a previous study [13]; the comparison reveals that the presence of the small particles in the mixture depresses the critical temperature significantly. Estimates of the phase boundary in $\mu_l - T$ space are shown in Fig. 4(b).

As regards the validation of our methodology, we have checked it by generating coexistence data for the same model using a simulation technique that operates along fundamentally different lines, namely the "GCA-RGE" simulation method of ref. [39]. Data for the coexistence densities of large particles were obtained for $T = 0.85$ and $T = 0.90$ and are included on Fig. 4 (crosses). Clearly the level of agreement is very high, which supports the correctness of our implementation.

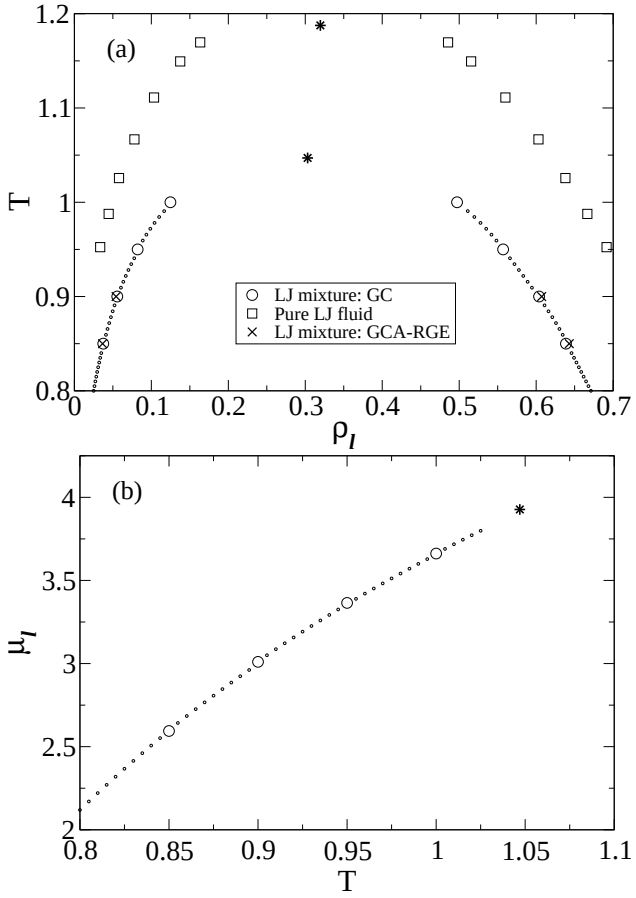

FIG. 4. **(a)** Coexistence densities (circles) as determined from the peak positions of Fig. 3; dots interpolate between the measured coexistence densities, and are determined via histogram reweighting. Squares show the binodal for the single component LJ fluid obtained in Ref. [13]. Critical points are marked (*). Crosses (×) are coexistence densities obtained using the GCA-RGE technique [39] as discussed in the text. Statistical uncertainties do not exceed the symbol sizes. **(b)** Corresponding coexistence points in the $\mu_l - T$ plane, with additional points (dots) obtained via histogram extrapolation.

We point out that obtaining this phase diagram in a

reasonable timescale would not have been feasible without the staged insertion/deletion approach. Our tests show that the wall clock correlation time in the absence of staging is too large to be reliably estimated. Nevertheless, a lower bound on the ratio of correlation times with and without staging can be estimated via a comparison of the transition acceptance rates. For $\eta_s^r = 0.01$, the insertion/deletion rate without staging is $\sim 10^{-6}$ at liquid-like densities of the large particles. This very low acceptance rate is of course attributable to the high likelihood that a randomly chosen large particle insertion results in overlaps with one or more small particles – a visual impression of the difficulty is provided by configurational snapshots of the coexisting phases as shown in Fig. 5. Use of staging increases the transition acceptance rate to $\sim 10^{-2}$ for $M = 4$ stages. The cost overhead is an increases in the (round trip) random walk length in N_l by a factor of M, thereby increasing the correlation time by a factor $M^2 \sim 10$. Hence we believe that in the present case our method is more efficient than standard grand canonical sampling by a net factor of $\sim 10^3$.

Notwithstanding the impressive scale of this speedup, the net computational expenditure incurred by our study remained significant. This is primarily due to the large number of small particles in the system, even for the relatively low volume fractions of small particles that we considered. To be more quantitative, the task of obtaining the initial multicanonical weight function consumed about a week of CPU time on a 32-core 3 GHz machine, while data collection for each subsequent coexistence state point also took about a week.

IV. CONCLUSIONS

In summary, we have described a grand canonical Monte Carlo simulation scheme for the study of fluid phase transitions in highly size-asymmetrical binary mixtures. The method overcomes the low acceptance rate for large particle transfers that plagues standard GC approaches. This is achieved via a staged insertion scheme whereby insertion (deletion) of a large particle proceeds stochastically via a set of intermediate states in which the coupling to the environment of small particles is switched on (off) gradually in stages. Once a suitable set of stages and associated multicanonical weights has been determined, the system essentially performs a random walk in the density of the large particles. We have applied the method to a particular binary Lennard-Jones mixture having $q = 0.1$ and $\eta_s^r = 1\%$, determining the coexistence envelope for liquid-vapour demixing of the large particles.

As regards the outlook for this approach, we see no reason why it shouldn't be effective at larger reservoir volume fractions of the small particles, or indeed for multicomponent mixtures. The principal computational overhead associated with higher values of η_s^r will be the larger number of interactions with small particles. The number of stages M necessary to maintain a reasonable acceptance rate will presumably increase too. We hope to investigate and report on these issues in future work.

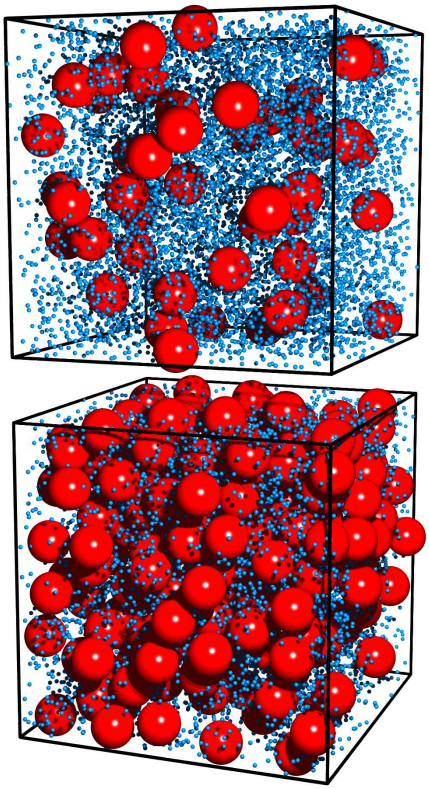

FIG. 5. Configuration snapshots of the coexisting vapour phase (upper panel) and liquid phase (lower panel) at $T^\star = 0.95$.

ACKNOWLEDGMENTS

It is a pleasure to contribute to this Special Issue of *Molecular Physics* celebrating the work of Professor Bob Evans. During his career, Bob has made numerous seminal contributions to liquid state theory, been a tireless champion of the field, and an inspiration to those in it. We wish him many rewarding years to come. This work was supported by EPSRC grant EP/F047800. Computational results were partly produced on a machine funded by HEFCEs Strategic Research Infrastructure fund.

[1] L. Belloni, J. Phys.: Condens. Matter **12**, R549 (2000).

[2] W.B. Russel, D.A. Saville, and W.R. Schowalter, *Colloidal Dispersions* (Cambridge U.P., Cambridge, 1989).

[3] W.C.K. Poon, J. Phys.: Condens. Matter **14**, R859 (2002).
[4] E. Zaccarelli *et al.*, Phys. Rev. Lett. **103**, 135704 (2009).
[5] J. Liu and E. Luijten, Phys. Rev. E **72**, 061401 (2005).
[6] L. Belloni, J. Phys. Condens. Matter **12**, R549 (2000).
[7] A. Ayadim and S. Amokrane, Phys. Rev. E **74**, 021106 (2006).
[8] P.N. Pusey, *Les Houches: Liquids, freezing and glass transitions* (North Holland, Amsterdam, 1991).
[9] S. Asakura and F. Oosawa, J. Chem. Phys. **22**, 1255 (1954).
[10] B. Götzelmann, R. Evans, and S. Dietrich, Phys. Rev. E **57**, 6785 (1998).
[11] M. Dijkstra, R. van Roij, and R. Evans, Phys. Rev. Lett. **81**, 2268 (1998).
[12] M. Dijkstra, R. van Roij, and R. Evans, Phys. Rev. E **59**, 5744 (1999).
[13] N. B. Wilding, Phys. Rev. E **52**, 602 (1995).
[14] N.B. Wilding and M. Muller, J. Chem. Phys. **101**, 4324 (1994).
[15] I. Nezbeda and J. Kolafa, Mol. Sim. **5**, 391 (1991).
[16] P. Attard, J. Chem. Phys. **98**, 2225 (1993).
[17] R. D. Kaminsky, J. Chem. Phys. **101**, 4986 (1994).
[18] D. Frenkel and B. Smit, *Understanding Molecular Simulation* (Academic, San Diego, 2002).
[19] K. K. Mon and R. B. Griffiths, Phys. Rev. A **31**, 956 (1985).
[20] F. A. Escobedo, J. Chem. Phys. **127**, 174104 (2007).
[21] W. Shi and E. J. Maginn, J. Chem. Theory Comp. **3**, 1451 (2007).
[22] A. P. Lyubartsev, A. A. Martsinovski, S. V. Shevkunov, and P. N. Vorontsov-velyaminov, J. Chem. Phys. **96**, 1776 (1992).
[23] B. A. Berg and T. Neuhaus, Phys. Rev. Lett. **68**, 9 (1992).
[24] Note that this volume fraction is notional in the sense that we use the value of σ as if it were a hard core radius $\eta_s = \pi N_s \sigma_s^3/(6V)$ where V is the system volume.
[25] We note in passing that further efficiency gains accrue by reducing the cell side by a factor of 2 and summing over a greater number of cells, thereby reducing the volume to be searched by up to a factor of 2.
[26] While certainly sufficient, this choice of weights is generally not *optimal* [27, 28].
[27] S. Trebst, D. A. Huse, and M. Troyer, Phys. Rev. E **70**, 046701 (2004).
[28] F.A. Escobedo and F.J. Martinez-Veracoechea, J. Chem. Phys. **129**, 154107 (2008).
[29] B. Berg, J. Stat. Phys. **82**, 323 (1996).
[30] G. R. Smith and A. D. Bruce, Phys. Rev. E. **53**, 6530 (1996).
[31] A. D. Bruce and N. B. Wilding, Adv. Chem. Phys **127**, 1 (2003).
[32] J.R. Errington, J. Chem. Phys. **120**, 3030 (2004).
[33] G.R. Smith and A.D. Bruce, J. Phys. A **28**, 6623 (1995).
[34] M. Fitzgerald, R. R. Picard, and R. N. Silver, Europhys. Lett. **46**, 282 (1999).
[35] In practice, the initial estimate of $w(N_l, n)$ can be obtained more rapidly by restricting the range of N_l that can be sampled in a given run. This is done by holding N_l inside a fixed window, $N_l^{\rm low} \leq N_l \leq N_l^{\rm high}$. The results from different windows can be combined self consistently by simply merging the collection matrix from each.
[36] A.M. Ferrenberg and R.H. Swendsen, Phys. Rev. Lett. **63**, 1195 (1989).
[37] N.B. Wilding, Am. J. Phys. **69**, 1147 (2001).
[38] C. Borgs and R. Kotecky, Phys. Rev. Lett. **68**, 1734 (1992).
[39] J. Liu, N.B. Wilding, and E. Luijten, Phys. Rev. Lett. **97**, 115705 (2006).